

Thermal Properties of Na₈ Microclusters

Aurel Bulgac and Dimitri Kusnezov^(a)

*National Superconducting Cyclotron Laboratory and Department of Physics and Astronomy,
Michigan State University, East Lansing, Michigan 48824-1321*

(Received 8 July 1991)

We present results of isothermal molecular-dynamics calculations for Na₈ microclusters. The Born-Oppenheimer dynamics is calculated using a many-body potential developed by Tománek and co-workers. We analyzed the system in a temperature range from 25 to 1500 K. The Na₈ cluster seems to undergo two phase transitions, a solid-glass transition at ≈ 100 K, and a melting transition at $T \approx 800$ K.

PACS numbers: 64.70.Dv, 64.70.Pf, 82.20.Fd, 82.20.Wt

The great interest in sodium microclusters [1] warrants a detailed understanding of their thermal behavior. In contrast to argon clusters, the thermal properties of alkali clusters do not seem to be a reflection of the underlying cluster geometry. The coexistence of solid-liquid phases in argon clusters was a property characteristic of certain numbers of atoms, and the addition or removal of a single atom resulted in a totally different phase diagram [2]. On the other hand, the aspect of the phase diagram for sodium clusters with different numbers of particles is qualitatively similar [3]. This is one of the reasons why we shall limit the present analysis to Na₈, and defer further details of this and other systems to future publications [3]. This cluster has been studied extensively, both experimentally and theoretically [1]. One of the main reasons is its magic character (electronic shell closure), which leads to an enhanced stability and therefore to a higher production rate. So far, a detailed study of the

thermal properties of alkali clusters, matching in detail the studies of argon clusters, is missing. In the case of noble gases, the interaction between atoms is relatively weak and also pairwise in character. This is not the case any more for metallic clusters, where the strong delocalization of the valence electrons leads to an effective Born-Oppenheimer interaction which is both relatively strong and many body in character. As we show below, these new features of the interaction lead to qualitatively new thermal behavior and a different phase diagram.

Ideally, an explicit treatment of ions and electrons in the framework of an *ab initio* molecular-dynamics study would be desirable [4]. However, the prohibitive amount of computation required suggests an implicit treatment of the electrons. The strong delocalization of the valence electrons in alkali clusters could be imitated by a many-body potential [5,6], used previously in the description of both bulk and clusters properties. The potential energy V of the sodium microcluster has the form [5,6]

$$V = \frac{E_{\text{coh}}}{(1-q/p)Z_b^{1/2}} \sum_{i=1}^N \left\{ \left\{ \sum_{j \neq i}^N \exp \left[-2q \left(\frac{r_{ij}}{r_0} - 1 \right) \right] \right\}^{1/2} - \frac{q}{pZ_b^{1/2}} \sum_{j=1}^N \exp \left[-p \left(\frac{r_{ij}}{r_0} - 1 \right) \right] \right\}.$$

The input parameters are [6] the bulk cohesive energy $E_{\text{coh}} = -1.113$ eV, the effective bulk coordination number $Z_b = 10.4$, the nearest-neighbor distance in the bulk $r_0 = 3.66$ Å, $p = 9$, and $q = 3$. The parameters of this interaction were derived from a tight-binding model, which reproduces reasonably well the binding characteristics of bulk sodium [2]. In spite of its simplicity, this interaction seems to describe surface properties extremely well [6]. Since clusters are mostly surface, one can reasonably expect that our results are not too far off the mark. A recent explicit treatment of the electrons at finite temperatures, within the framework of a tight-binding Hamiltonian for Cu clusters [7], points to a remarkable stability of the electronic shell structure even at relatively high temperatures. This result, expected from general physical arguments, lends support to the use at finite temperatures of the effective Born-Oppenheimer interaction derived at $T = 0$ (at least for magic clusters). In particular, the interaction used here seems to describe reasonably well the

structure of the Na₈ ground state.

The canonical ensemble can be generated either in a standard Monte Carlo technique or better in the hybrid Monte Carlo method [8]. We have chosen to use our improved Nosé-Hoover type of molecular dynamics (MD) [9], which showed better convergence properties in the case of the XY model than did the hybrid Monte Carlo method [10]. The coupling to a thermostat at absolute temperature T ($k_B = 1$) was described by the following equations of motion [5,6]:

$$\dot{x}_i = \frac{p_{xi}}{m} - \bar{\beta} \xi_x \left(x_i^3 - \frac{1}{N} \sum_{k=1}^N x_k^3 \right),$$

$$\dot{p}_{xi} = - \frac{\partial V}{\partial x_i} - \bar{\alpha} \zeta_x^3 \left(p_{xi} - \frac{1}{N} \sum_{k=1}^N p_{xk} \right),$$

for the coordinates (x_i, y_i, z_i) and momenta (p_{xi}, p_{yi}, p_{zi})

of each atom $i=1, \dots, N$, and

$$\xi_x = \beta \bar{\beta} \sum_{i=1}^N \left(\frac{\partial V}{\partial x_i} x_i^3 - 3 \frac{N-1}{N} T x_i^2 \right),$$

$$\zeta_x = \alpha \bar{\alpha} \left[\sum_{i=1}^N p_{x_i}^2 - (N-1)T \right],$$

for the pseudofriction coefficients (ξ_x, ξ_y, ξ_z) and $(\zeta_x, \zeta_y, \zeta_z)$. This type of coupling does not affect the center-of-mass motion. We have introduced a pair of pseudofriction coefficients for each Cartesian component in order to avoid the conservation of the total angular momentum (or its direction) and to ensure ergodicity and a higher rate of exploration of the cluster internal phase space. The constants $\alpha, \bar{\alpha}, \beta, \bar{\beta}$ control the energy exchange rate between the cluster and the bath. They were chosen to optimize the convergence of the procedure by varying them with T . The equations of motion were integrated using a Hamming predictor-corrector method of fourth order. The time step was chosen between 0.15×10^{-15} and 2×10^{-15} s, depending on temperature (smaller steps for higher T) and 10^6 configurations were generated at each temperature. This resulted in relatively long time simulations, between 0.12 and 2 ns, which allowed us to extract rather detailed information. In order to avoid evaporation at high T we have added a linear restoring force at $r_{ij} \geq 22 \text{ \AA}$.

A very sensitive "phase transition gauge" is the dimensionless bond-length fluctuation [2]

$$\delta = \frac{2}{N(N-1)} \sum_{i < j}^N \frac{(\langle r_{ij}^2 \rangle - \langle r_{ij} \rangle^2)^{1/2}}{\langle r_{ij} \rangle}.$$

At low temperatures, the atoms oscillate with small amplitudes around their equilibrium positions. At a temperature of about 100 K, the bond-length fluctuation jumps from almost 0 to about 0.3 (see Fig. 1), similar to the case of argon clusters [2] and other metal clusters [5]. At these temperatures the atoms are oscillating most of the time with small amplitudes around the equilibrium position and once in a while some of them jump to other equilibria. A similar phenomenon was observed for the gold clusters [11] and this phase was characterized as a "glassy" or "molten state" of the cluster. At temperatures corresponding to the second "phase transition," there is another dramatic increase in the bond-length fluctuation to a value of about 0.5. The cluster becomes fluidlike and all the atoms move across the entire cluster. At the same time there is a significant evaporation probability.

We monitored the total kinetic energy of the cluster mostly as a check of our simulation procedure, since quantities like the average kinetic energy, kinetic specific heat, and the shape of the kinetic-energy distribution itself can be predicted beforehand. The kinetic energy can be separated into two nontrivial contributions however: rotational and vibrational energies [12]. In the whole

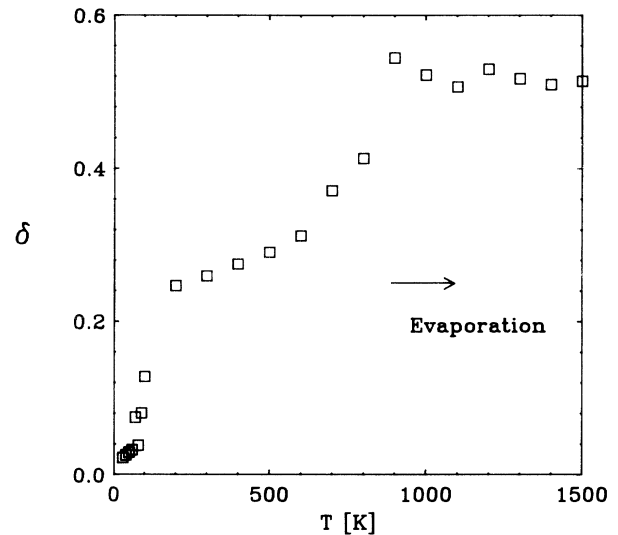


FIG. 1. The temperature dependence of the bond-length fluctuation δ in a Na_8 microcluster. This quantity displays distinct jumps at the two phase transitions.

range of temperatures studied, the average rotational energy and the corresponding contribution to the specific heat are, within statistical errors, the same as for a rigid body, in spite of the floppiness of the cluster [12]. For temperatures below ~ 35 K the cluster behaves like an ensemble of harmonic oscillators. The potential-energy contribution to the specific heat is essentially that given by the equipartition formula for independent oscillators, i.e., $C_{\text{pot}} = (3N-6)/2 = 9$. The configuration of the

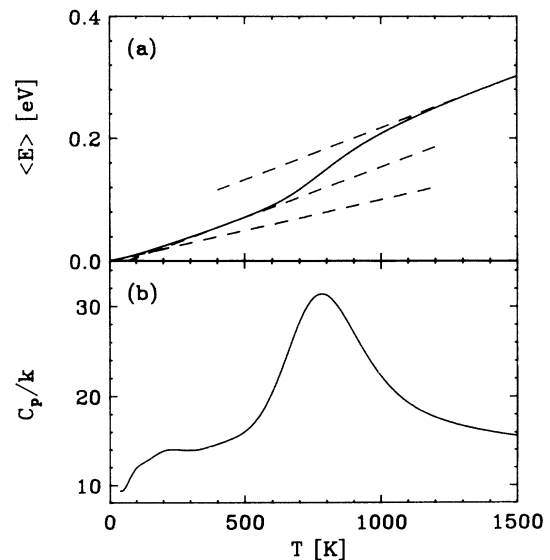


FIG. 2. (a) The temperature dependence of the average potential energy. The dashed lines are guides to the eye and give an idea about the slopes of the average potential energy in different temperature intervals. (b) The potential-energy contribution to the specific heat.

ground state is very similar to the D_{2d} isomer [13], corresponding to a prolate rotor. At much higher temperatures, $T \approx 800$ K, there is another much better defined jump in the specific heat, which can be seen in the plot of the average potential energy as a function of temperature as well (Fig. 2).

The distribution of the potential energy at a given temperature is $P(E) = \rho(E)\exp(-E/T)/Z(T)$, where $Z(T)$ is the partition function and $\rho(E)$ is the density of states. Since our calculation determines the energy distribution directly, we can determine the density of states $\rho(E)$ from the computed $P(E)$, up to an arbitrary normalization constant. This constant can be computed in a variety of ways: either using a harmonic approximation around the ground state or by the adiabatic switching method [14]. Patching together different pieces obtained at different T , we defined $\rho(E)$ over a large interval and subsequently determined the partition function, entropy, average energy, and specific heat as functions of T . We found that the curvature of $\log_{10}\rho(E)$ becomes positive for some energies (see Fig. 3), a behavior characteristic only of small systems [15]. This behavior of the density of states as a function of energy is responsible for the occurrence of a bimodal energy distribution at certain temperatures (see inset of Fig. 3), and the so-called coexistence of phases [2].

For each spatial configuration one can compute the principal moments of inertia $I_1 \geq I_2 \geq I_3 \geq 0$. They provide average information about the shape and size of the cluster; see Fig. 4. The three principal (geometrical) moments of inertia can be used to compute β (which characterizes the degree of nonsphericity) and γ (which gives a measure of the triaxiality) parameters [3]. We have

chosen the following definition of these parameters:

$$I_k = \frac{2}{3} r^2 \left[1 + \beta \sin \left[\gamma + \frac{(4k-3)\pi}{6} \right] \right],$$

$$k = 1, 2, 3, \quad I_1 + I_2 + I_3 = 2r^2,$$

where $r = (\sum_{i=1}^N r_i^2 / N)^{1/2}$ ($\sum_{i=1}^N r_i = 0$) is the rms radius of the matter distribution. The condition that the semi-minor axis $a^2 = (r^2/3)[1 - 2\beta \sin(\gamma + \pi/6)] \geq 0$ defines the region of allowed values for β and γ . At low temperatures, the cluster has a rather well-defined rms radius. The cluster is essentially incompressible, but can deform quite easily (see Fig. 4), which is a consequence of the s character of the bonding. At higher temperatures the rms radius of the cluster has a quite broad distribution and at the same time its average value rises sharply around 800 K. Above 800 K, the cluster has a cigarlike shape with a sizable triaxial deformation. The smallest moment of inertia has the biggest fluctuations. This means that atoms evaporate most willingly from the sides of the cigar.

In conclusion, the partial results presented here suggest that the phase diagram of sodium clusters, in spite of many similarities with Lennard-Jones clusters, is more complicated. In this case, there are two clearly distinguishable "phase transitions," one from a solid to a glass or molten state and the other one to a fluid state. Both energetic and geometric properties of the cluster undergo significant changes with temperature. It is reasonable to conclude that mainly the many-body character of the in-

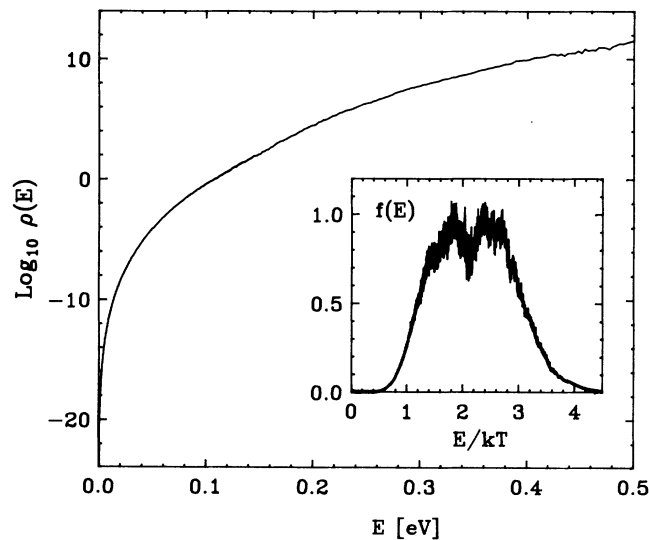


FIG. 3. The density of states $\rho(E)$ (potential energy only) extracted from isothermal MD calculations and a bimodal potential-energy distribution for Na_8 at $T = 820$ K.

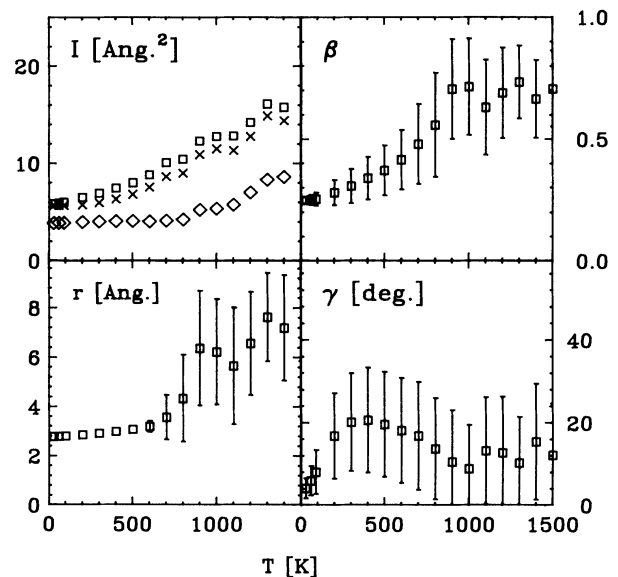


FIG. 4. The temperature dependence of the averaged three principal moments of inertia, the rms radius together with its width, and the shape parameters β and γ . The widths of the corresponding distributions (covariance) are plotted as error bars.

teraction among the sodium atoms is responsible for the marked differences with Lennard-Jones clusters. A more detailed exposure of the present results along with properties of other sodium clusters will be presented elsewhere [3].

We thank D. Tománek and G. F. Bertsch for extensive discussions and suggestions. Support was provided by NSF under Grants No. 89-06670 and No. 90-17077.

^(a)Permanent address: Center for Theoretical Physics, Sloane Laboratory, Yale University, New Haven, CT 06511.

- [1] W. A. De Heer, W. D. Knight, M. Y. Chou, and M. L. Cohen, in *Solid State Physics*, edited by H. Ehrenreich and D. Turnbull (Academic, New York, 1987), Vol. 40, p. 93.
- [2] R. S. Berry, T. L. Beck, H. L. Davis, and J. Jellinek, *Adv. Chem. Phys.* **70**, 75 (1988); H. L. Davis, J. Jellinek, and R. S. Berry, *J. Chem. Phys.* **86**, 6456 (1987).
- [3] A. Bulgac and D. Kusnezov, *Phys. Rev. B* **45**, 1988 (1992); N. Ju and A. Bulgac (to be published).
- [4] P. Ballone, W. Andreoni, R. Car, and M. Parrinello, *Europhys. Lett.* **8**, 73 (1989).
- [5] S. Sawada and S. Sugano, *Z. Phys. D* **14**, 247 (1989); J. Jellinek and I. L. Garzon, *Z. Phys. D* **20**, 239 (1991); I. L. Garzon and J. Jellinek, *Z. Phys. D* **20**, 235 (1991).
- [6] D. Tománek and K. H. Bennenmann, *Surf. Sci.* **163**, 503 (1985); D. Tománek, S. Mukherjee, and K. H. Bennenmann, *Phys. Rev. B* **28**, 665 (1983); **29**, 1076(E) (1984); D. Tománek, A. A. Aligia, and C. A. Balseiro, *Phys. Rev. B* **32**, 5051 (1985); W. Zhong, Y. S. Li, and D. Tománek, *Phys. Rev. B* **44**, 13053 (1991).
- [7] O. B. Christensen, K. W. Jacobsen, J. K. Nørskov, and M. Maninen, *Phys. Rev. Lett.* **66**, 2219 (1991).
- [8] S. Duane, A. D. Kennedy, B. J. Pendleton, and D. Roweth, *Phys. Lett. B* **195**, 216 (1987); A. D. Kennedy and B. Pendleton, *Nucl. Phys.* **B20**, 118 (1991), and references therein.
- [9] A. Bulgac and D. Kusnezov, *Phys. Rev. A* **42**, 5045 (1990); D. Kusnezov, A. Bulgac, and W. Bauer, *Ann. Phys. (N.Y.)* **204**, 155 (1990); A. Bulgac and D. Kusnezov, *Phys. Lett. A* **151**, 122 (1990); D. Kusnezov and A. Bulgac, *Ann. Phys. (N.Y.)* (to be published).
- [10] J. H. Sloan, D. Kusnezov, and A. Bulgac, in *Proceedings of the Conference on Computational Quantum Physics*, Nashville, 23–25 May 1991, edited by C. Bottcher *et al.* (AIP, New York, to be published).
- [11] S. Iijima and T. Ichihashi, *Phys. Rev. Lett.* **56**, 616 (1986); P. M. Ajayan and L. D. Marks, *Phys. Rev. Lett.* **60**, 585 (1988); **63**, 279 (1989).
- [12] J. Jellinek and D. H. Li, *Phys. Rev. Lett.* **62**, 241 (1989); J. Jellinek and P. G. Jasien, in *The Structure of Small Molecules and Ions*, edited by R. Naaman and Z. Vager (Plenum, New York, 1989), p. 39; D. H. Li and J. Jellinek, *Z. Phys. D* **12**, 177 (1989).
- [13] I. Moullet, J. L. Martins, F. Reuse, and J. Buttet, *Phys. Rev. Lett.* **65**, 476 (1990).
- [14] W. Masakatsu and W. P. Reinhardt, *Phys. Rev. Lett.* **65**, 3301 (1990).
- [15] P. Labastie and R. L. Whetten, *Phys. Rev. Lett.* **65**, 1567 (1990); R. Kubo, *Statistical Mechanics* (North-Holland, Amsterdam, 1965), Chap. 1.